Increased ^{18}F-Fluorodeoxyglucose Uptake in Benign, Nonphysiologic Lesions Found on Whole-Body Positron Emission Tomography/Computed Tomography (PET/CT): Accumulated Data From Four Years of Experience With PET/CT

Ur Metser, MD,*,†,‡ and Einat Even-Sapir, MD, PhD*,‡

The use of ^{18}F-fluorodeoxyglucose positron emission tomography (^{18}F-FDG-PET) in the field of oncology is rapidly evolving; however, ^{18}F-FDG is not tumor specific. Aside from physiological uptake ^{18}F-FDG also may accumulate in benign processes. Knowledge of these ^{18}F-FDG-avid nonmalignant lesions is essential for accurate PET interpretation in oncologic patients to avoid a false-positive interpretation. Through the systematic review of the reports of PET/computed tomography (CT) studies performed in oncologic patients during a 6-month period, we found benign nonphysiological uptake of ^{18}F-FDG in more than 25% of studies. In half of these, ^{18}F-FDG uptake was moderate or marked in intensity, similar to that of malignant sites. A total of 73% of benign lesions were inflammatory in nature, with post-traumatic bone and soft-tissue abnormalities (including iatrogenic injury) and benign tumors accounting for the remainder. The differentiation of benign from malignant uptake of ^{18}F-FDG on PET alone may be particularly challenging as a result of the low anatomical resolution of PET and paucity of anatomical landmarks. Fusion imaging, namely PET/CT, has been shown to improve not only the sensitivity of PET interpretation but also its specificity. Aside from better anatomical localization of lesions on PET/CT, morphological characterization of lesions on CT often may improve the diagnostic accuracy of nonspecific ^{18}F-FDG uptake. Correlation with CT on fused PET/CT data may obviate the need for further evaluation or biopsy in more than one-third of scintigraphic equivocal lesions. Familiarity with ^{18}F-FDG-avid nonmalignant lesions also may extend the use of ^{18}F-FDG-PET imaging beyond the field of oncology. We have tabulated our experience with benign entities associated with increased ^{18}F-FDG uptake on whole-body PET/CT from 12,000 whole-body ^{18}F-FDG-PET/CT studies performed during a 4-year period.
Semin Nucl Med 37:206-222 © 2007 Elsevier Inc. All rights reserved.

The use of ^{18}F-fluorodeoxyglucose positron emission tomography (^{18}F-FDG-PET) in various malignancies is rapidly evolving; however, ^{18}F-FDG uptake is not tumor specific. Aside from physiological uptake in Waldeyer's ring, the gastrointestinal tract, orbital muscles, cerebral cortex, myocardium, renal collecting systems, bladder, gonads, and brown fat, ^{18}F-FDG also may accumulate in benign processes, the majority of which are inflammatory.[1,2] Knowledge of these potentially false-positive lesions is essential for accurate PET interpretation in oncologic patients.

Recently, a systematic review of PET/computed tomography (CT) studies was performed in oncologic patients during a 6-month period and has shown that benign, nonphysiological uptake of ^{18}F-FDG is encountered in more than 25% of studies. In more than half of them, ^{18}F-FDG uptake may be moderate or marked as compared with background activity. More than 73% of benign lesions were inflammatory in nature, with post-traumatic bone and soft-tissue abnormalities

*Department of Nuclear Medicine, Tel-Aviv Sourasky Medical Center, Tel-Aviv, Israel.
†Department of Radiology, Tel-Aviv Sourasky Medical Center, Tel-Aviv, Israel.
‡Sackler Faculty of Medicine, Tel-Aviv University, Tel-Aviv, Israel.
Address reprint requests to Einat Even-Sapir, MD, PhD, Department of Nuclear Medicine, Tel-Aviv Sourasky Medical Center, 6 Weizman Street, Tel-Aviv 64239, Israel. E-mail: evensap@tasmc.health.gov.il

Table 1 Inflammatory Lesions Showing Increased Uptake of ^{18}F-FDG in the Head and Neck Region

Location	Lesion Type
Sinonasal cavity	Sinusitis
Ear and mastoid	Otitis, mastoiditis
Mouth, pharynx, and larynx	Dental abscess, pharyngitis, tonsillitis, rheumatoid nodule in paraepiglottic space
Salivary glands	Sialadenitis

(including iatrogenic injury) in addition to benign tumors accounting for most of the remaining lesions.[3] Differentiating benign from malignant uptake of ^{18}F-FDG on PET alone may be particularly challenging because of the low anatomical resolution of PET and paucity of anatomical data. Fusion imaging, namely PET/CT, has been shown to improve not only the sensitivity of PET interpretation but also its specificity.[4,5] Aside from better anatomical localization of lesions on PET/CT, morphological characterization on CT often may improve the diagnostic accuracy of nonspecific ^{18}F-FDG avid lesions.[5-7] A confident benign diagnosis can often be made with CT correlation on fused PET/CT, obviating the need for further evaluation or biopsy in over a third of lesions.[3]

Data regarding benign lesions showing an abnormal uptake of [18]F -FDG are sporadic in the literature and mainly are found in the form of case reports. We have tabulated our experience with benign entities associated with increased ^{18}F-FDG uptake on whole-body PET/CT from more than 12,000 whole-body ^{18}F-FDG-PET/CT scans performed during a 4-year period.

^{18}F-FDG Uptake in Inflammation: Pathophysiology

Inflammation is the primary response of the immune system to infection or irritation, as well as to trauma. In response to these stimuli, a cascade of events occurs, including local hyperemia, release of proteins such as fibrin and immunoglobulins, leakage of fluids, and infiltration of inflammatory cells.[8] Increased uptake of ^{18}F-FDG in inflammation may be explained by the recruitment of activated white blood cells (granulocytes, lymphocytes, and macrophages), which have enhanced levels of glucose transporters, especially GLUT 3 and GLUT 1,[9] as well as increased affinity to ^{18}F-FDG

through various cytokines and growth factors. One such cytokine is tumor necrosis factor-α, produced primarily by monocytes, which has been shown to activate macrophages in experimental models of inflammation as well as clinically in rheumatoid arthritis or in response to bacterial endotoxins.[10,11] Activated monocytes directly activate reduced nicotinamide adenine dinucleotide phosphate (NADPH) oxidase, which imposes an acute metabolic demand met by an increased use of both internal energy stores and exogenous metabolites such as glucose.[12,13] Recently, in vitro studies have shown that the activation of monocytes, without further activation of NADPH oxidase, is sufficient to increase glucose metabolism.[12] These pathophysiologic processes are the basis for increased uptake of ^{18}F-FDG that is encountered in acute inflammatory processes. Although uptake of ^{18}F-FDG in inflammation may cause false-positive PET interpretation in oncology patients, it may be exploited to assess inflammation.

^{18}F-FDG-PET has been used to assess the activity of inflammatory disease and response to therapy in several diseases such as sarcoidosis and vasculitis.[14,15] In patients with large-vessel vasculitis, ^{18}F-FDG uptake has been shown to correlate well with the level of acute phase reactant markers and thus with activity of inflammation.[15] Even in the presence of severe immunosuppression, ^{18}F-FDG-PET can detect the presence and extent of infectious foci not identified with conventional diagnostic methods, even when clinically silent. Therefore, PET may lead to modifications in the therapeutic strategy in this clinical scenario.[16]

Infection and Inflammation

Head and Neck

Infections in the head and neck region are common and may involve the sinonasal cavities, pharynx, tonsils, ears, and mastoids (Table 1). As a general rule of thumb, acute inflammatory processes tend to show greater intensity of ^{18}F-FDG uptake than chronic processes. Occasionally, it may be impossible to differentiate malignancy from inflammation (Fig. 1). In these cases, clinical correlation with close imaging follow-up may be useful. In other clinical instances, especially when the patient's primary malignancy is not in the head and neck region, a benign diagnosis can be suggested based on an unusual location for metastatic involvement, or
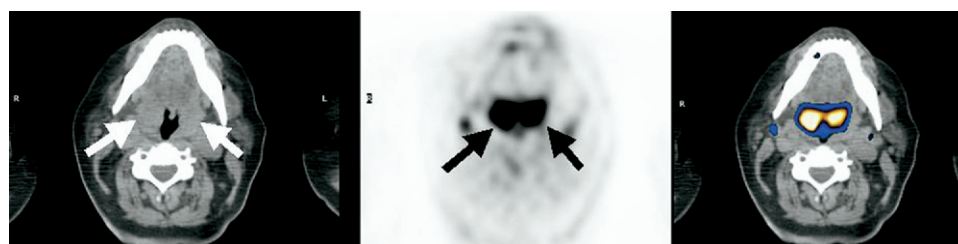

Figure 1 Acute tonsillitis. PET/CT axial image (CT on left, PET in middle, and fused PET/CT on right) of patient with acute follicular tonsillitis. Abnormal uptake of FDG is observed in both palatine tonsils (arrows), as well as in reactive jugulo-digastric lymph nodes.
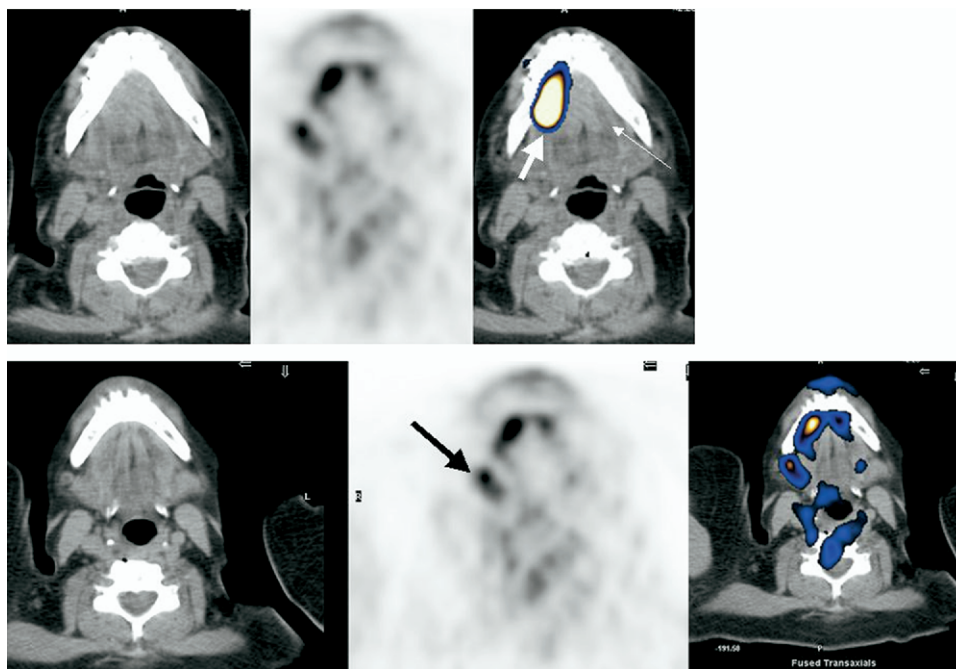
Figure 2 Sialadenitis. PET/CT axial images (CT on left, PET in middle, and fused PET/CT on right). Top row, abnormal uptake of FDG is seen in large squamous cell carcinoma of right tongue (long arrow on fused PET/CT image), involving region of right Wharton's duct. Note the uninvolved left Wharton's duct on CT image (thin arrows). Bottom row, Moderate asymmetrical uptake of FDG is noted in right submandibular salivary gland, caused by obstructive sialadenitis.

when there is a clear difference in FDG-avidity of the known malignancy and an incidental lesion.

Inflammatory disorders of the salivary glands may be infectious (viral or bacterial), granulomatous (typical or atypical mycobacterial infection, sarcoidosis, Wegner's granulomatosis), autoimmune (Sjogren's syndrome), or secondary to obstruction (Fig. 2).[17] Uptake of ^{18}F-FDG in salivary glands also may be iatrogenic. Inclusion of the salivary glands in an irradiation field may result in disruption of serous acini, which are extremely radiosensitive, with leakage of enzymes into the surrounding salivary tissues results in an acute inflammatory process. In general, uptake of ^{18}F-FDG in radiation field may be of high intensity within the first few weeks of radiation therapy as the result of inflammation; therefore, it is recommended to postpone restaging until 4 to 8 weeks from completion of radiation therapy, if clinically possible.[18]

Chest

As previously described in the literature, inflammatory pulmonary lesions may show increased uptake of ^{18}F-FDG (Fig. 3; Table 2).[19] When uptake is focal, it may be indistinguishable on PET from that of a primary or secondary neoplastic lesion (Fig. 3A). However, some lesions may be characterized as benign based on their appearance on CT. Lipoid pneumonia is a rare type of pneumonia caused by aspiration of mineral, vegetable, or animal oils, usually secondary to neuromuscular disorders associated with dysphagia. The characteristic histological features include lipid-laden macrophages in the alveolar walls and lung interstitium, with associated inflammation and fibrosis. On CT, a low-attenuation

nodule, mass, or consolidation with regions of fat-attenuation is suggestive of this entity.[20] Increased uptake of ^{18}F-FDG has been previously described, likely the result of an abundance of activated macrophages (Fig. 3B).[21]

Similarly, pulmonary Langerhans cell histiocytosis, an isolated form of histiocytosis X, which primarily affects smokers, may be associated with increased uptake of ^{18}F-FDG. A typical CT appearance is that of pulmonary cysts and nodules predominantly affecting the upper and midlung zones. Early in the course of disease, a predominantly nodular pattern may be encountered, whereas variably shaped cysts are typical of progressive disease.[22]

At times, although not pathognomonic, the CT imaging pattern may be suggestive of a specific diagnosis. Lung infarction secondary to pulmonary embolism may be an additional pitfall on ^{18}F-FDG-PET, especially in patients with malignancy who are at risk for thromboembolism. In our experience, pulmonary infarcts showed only mild uptake of ^{18}F-FDG, not posing a major diagnostic dilemma. However, uptake may be moderate or marked and may mimic malignancy.[23] In the appropriate clinical setting, a wedge-shaped peripheral region of consolidation on CT should raise the possibility of a pulmonary infarct (Fig. 3C).

Drug-induced lung toxicity is a relatively frequent complication in oncologic patients, with multiple cytotoxic drugs implicated (Fig. 4A). The clinical presentation and imaging findings depend on the pathologic processes induced by these drugs, which may include interstitial pneumonitis, diffuse alveolar damage, hemorrhage, edema, and cryptogenic organizing pneumonia (COP; previously known as bronchi-
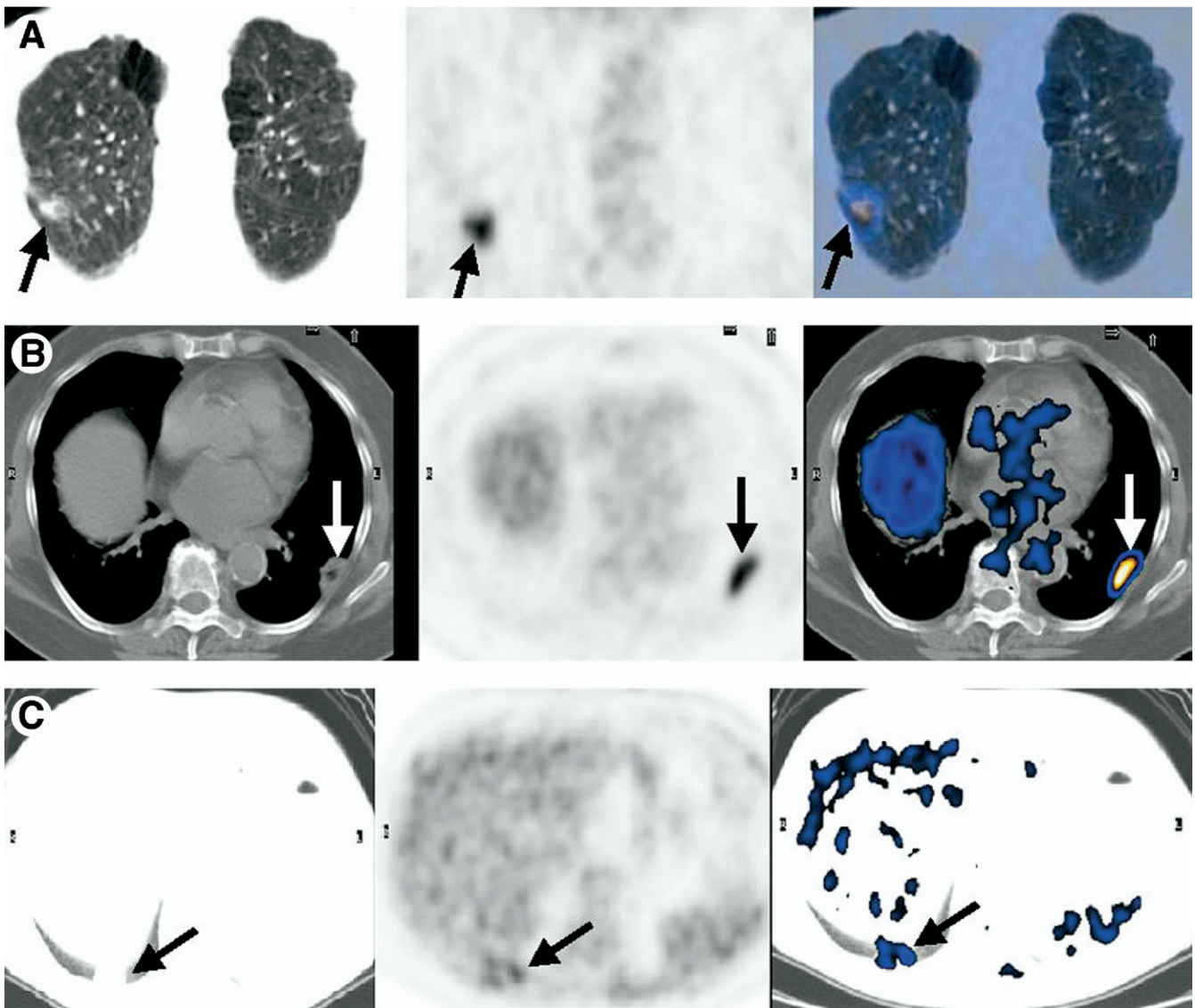
Figure 3 PET/CT patterns of benign lung lesions. (CT on left, PET in middle, and fused PET/CT on right). (A) Nonspecific PET/CT pattern. Marked uptake of FDG is found in a spiculated mass in right lung apex, indistinguishable from malignancy. On pathology, findings were consistent with active pulmonary tuberculosis. (B) Specific PET/CT pattern. Marked uptake of FDG is seen in subpleural mass. On CT, center of mass is fat-attenuating, consistent with lipoid pneumonia (confirmed histologically). (C) Suggestive PET/CT pattern. Mild-to-moderate uptake of FDG is seen in wedge-shaped pulmonary infiltrate, confirmed as pulmonary infarction on contrast-enhanced CT.

olitis obliterans with organizing pneumonia, or BOOP), among others.[24] Histologically, COP is characterized by the proliferation of immature fibroblastic plugs within respiratory bronchioles, alveolar ducts, and adjacent alveolar spaces. Aside from drug therapy, it may be anteceded by previous lung infection, or may be seen in patients with collagen vascular disease. Case reports have shown that increased 18F-FDG uptake may be associated with COP,[25] as was also found in our experience (Fig. 4B). On CT, consolidation involving subpleural and peribronchial areas are the most common finding, followed by ground-glass opacity and nodules.[26] Although none of these features is pathognomonic, in the appropriate clinical setting, when abnormal uptake of FDG is observed in such pulmonary findings on CT, drug toxicity or COP should be considered.

Table 2 Inflammatory Lesions Showing Increased Uptake of 18F-FDG in the Chest

Location	Lesion Type
Tracheobronchial tree	Tracheitis, infected bronchiectasis
Lung	Viral, bacterial, fungal infection, abscess, ILD, COP, lipoid pneumonia, Langerhans cell histiocytosis, vasculitis, sarcoidosis, Wegner's granulomatosis, inhalational lung disease
Pleura	Empyema
Breast	Infected cyst (fibrocystic disease), fat necrosis, leaking breast implant

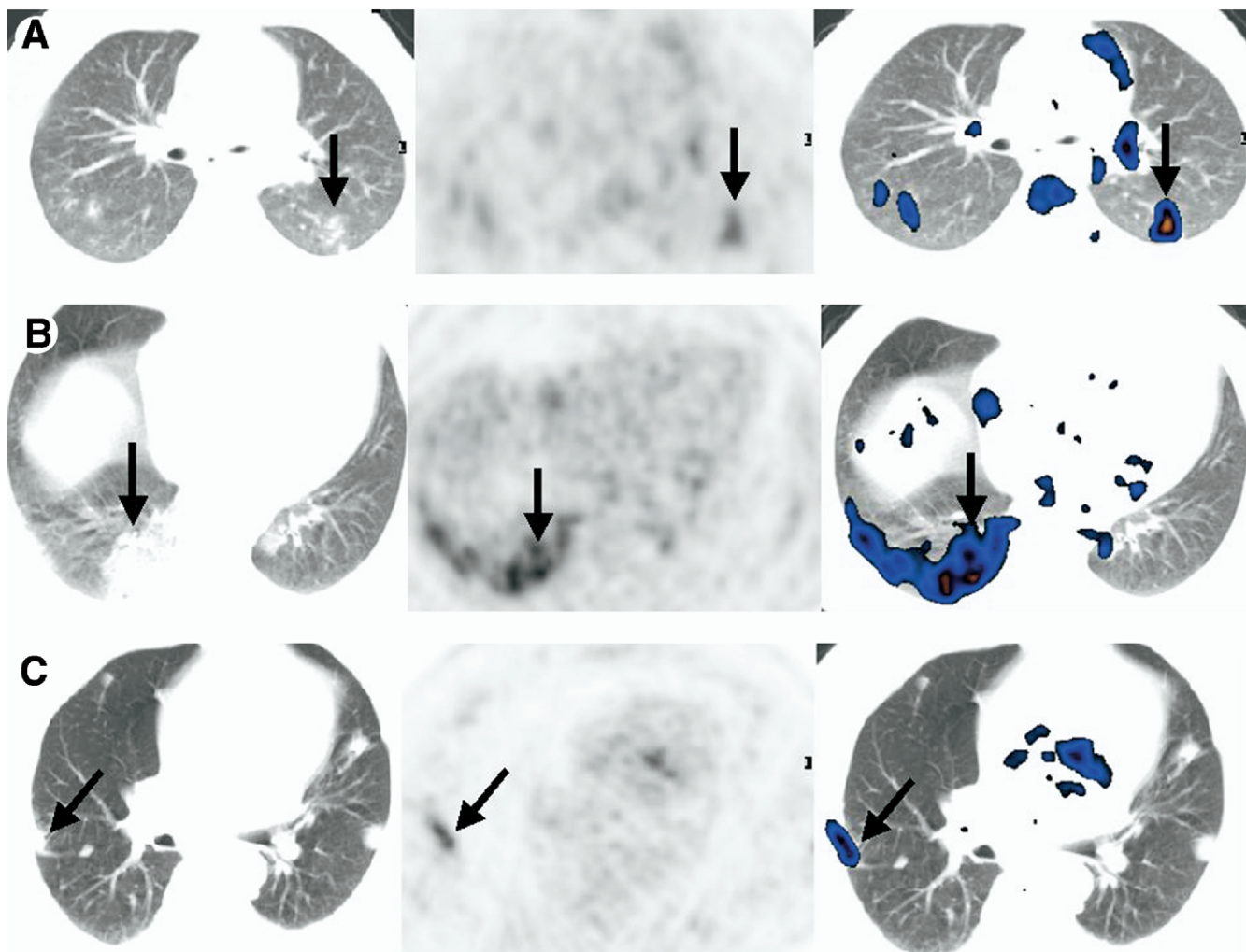ILD, interstitial lung disease; COP, cryptogenic organizing pneumonia.

Figure 4 Interstitial pneumonitides (CT on left, PET in middle, and fused PET/CT on right). (A) Bleomycin-induced pneumonitis. Moderate uptake of FDG is seen in multiple pulmonary nodules consistent with drug toxicity to bleomycin. (B) COP. Abnormal uptake of FDG in subpleural lung consolidations (arrows). (C) Lymphocytic interstitial pneumonitis (LIP). CT image shows multiple lung nodules, some showing abnormal uptake of FDG (solid arrow). Biopsy showed interstitial infiltrate of mononuclear cells, mixed with plasmocytes and histiocytes, suggestive of LIP.

Aside from COP, idiopathic interstitial pneumonitides include usual interstitial pneumonitis, nonspecific interstitial pneumonitis, desquamative interstitial pneumonitis, respiratory bronchiolitis-associated interstitial lung disease, acute interstitial pneumonitis, and lymphoid interstitial pneumonitis. Lymphoid interstitial pneumonitis results from progressive alveolocapillary block caused by nodular lymphoid hyperplasia and lymphocytic infiltrate in the interlobular and interalveolar septa and may be secondary to a variety of immunologic and autoimmune diseases (Fig. 4C).

Imaging findings in these disorders are nonspecific and may be identical to those found in other conditions, including collagen vascular disease or inhalational exposure.[27] Recently, it has been shown that ^{18}F-FDG-PET may be helpful in the evaluation of idiopathic interstitial pneumonitides. Increased activity on PET may suggest active disease, and a decrease in ^{18}F-FDG uptake correlates with response to therapy.[28] Radiation pneumonitis may occur 2 to 6 months after completion of radiation therapy in 2 separate phases: acute

pneumonitis and chronic lung fibrosis. The acute phase is characterized by loss of type I pneumocytes, increased capillary permeability and edema, and inflammation within alveolar spaces. This phase occurs when radiation therapy exceeds a threshold dose. Usually, radiation pneumonitis is limited to the radiation field. On PET/CT, a sharp linear demarcation is seen separating inflamed and normal lung tissue, suggestive of this entity. Later, pulmonary fibrosis may follow, with concomitant decrease in uptake of ^{18}F-FDG. Recently, increased metabolic activity on ^{18}F-FDG-PET has been demonstrated in nonirradiated lung fields as well as along pleural surfaces.[29] The mechanism for this is not well understood, but it has been postulated that radiation-induced damage may begin in the pleura.

Abdomen and Pelvis
Gastrointestinal Tract (Table 3)
Physiological uptake of ^{18}F-FDG along the gastrointestinal tract is variable among patients. Most often it is observed in

Table 3 Inflammatory Lesions Showing Increased Uptake of 18F-FDG Along the Gastrointestinal Tract

Location	Lesion Type
Nonspecific inflammation	Esophagitis, gastritis, gastric ulcer, enterocolitis, appendicitis, diverticulitis, inflammatory bowel disease (Crohn's disease, UC), perianal fistula
Infection	Typhlitis
Post-therapy inflammation	Acute radiation enterocolitis, pouchitis, graft-versus-host disease

UC, ulcerative colitis.

the gastro-esophageal junction, ileocecal valve region, and right colon, but at times, it may be all along the small and large intestine. The origin of 18F-FDG uptake in the digestive tract is unknown; however, possible causes that have been suggested are active smooth muscle, metabolically active mucosa, or swallowed secretions. Segmental uptake, especially when associated with bowel wall thickening with or without stranding of adjacent mesenteric fat on CT, may suggest focal inflammation.[30] These findings may be observed anywhere along the gastrointestinal tract. Direct correlation with CT may correctly suggest acute diverticulitis (Fig. 5A), acute appendicitis, or active inflammatory bowel disease (Fig. 5B). However, at times, only endoscopy and biopsy may exclude malignancy (Fig. 5C).

Immunocompromised patients are prone to bowel infections such as typhlitis (neutropenic enterocolitis) after antitumoral therapy. Typhlitis is an uncommon complication of stem cell transplantation involving the distal ileum and right colon, or may occur in other immunosuppressed patients such as those with leukemia (Fig. 6A). Edema and severe inflammatory changes in bowel wall may result in bowel perforation. At CT, cecal distention and circumferential thickening of the bowel wall are hallmark findings. Bowel wall thickening may have low attenuation secondary to submucosal edema. Inflammatory stranding of the adjacent mesenteric fat is a common accompanying finding. Detection of complications on the CT portion of the PET/CT study such as pneumatosis or pneumoperitoneum is important because it indicates bowel ischemia/infarction and bowel perforation, respectively, and a need for urgent surgical management.[31] These can be visualized.

Allogeneic stem cell transplant recipients are at risk for developing graft versus host disease (GVHD), a morbid clinical condition. Acute GVHD usually develops within the first 3 months after transplantation and is usually preceded by the development of a maculopapular rash. Although any part of the gastrointestinal tract may be involved, the most common segments of bowel to be affected are the small bowel and colon. Denuded gastrointestinal mucosa is replaced by granulation tissue. On CT, the characteristic findings are hyperemic bowel mucosa surrounded by lower-attenuation outer

bowel wall layers ("target sign"), bowel loop separation, and mesenteric fat stranding.[32] Imaging findings overlap with those of infectious processes involving the bowel. Because therapy for GVHD includes the use of immunosuppressive drugs, tissue sampling often is necessary to make a definitive diagnosis and exclude infection. The chronic form of GVHD occurs 3 or more months after transplantation, is a major cause of late morbidity and mortality, and is a major risk factor for late infection (Fig. 6B). In our experience, on 18F-FDG-PET/CT, low-intensity uptake of 18F-FDG in thickened loops of bowel may be encountered. These findings, along with an appropriate clinical history, may assist in making an accurate diagnosis.

Liver, Gallbladder, Biliary Tract, Pancreas, Spleen and Peritoneum (Table 4)

Liver abscesses may be classified as pyogenic, fungal, or parasitic. Liver infection may result from dissemination of organisms from a gastrointestinal infection via the portal vein, as is the case in amebic hepatic abscess,[33] or from sepsis via the hepatic artery, as is the case with most fungal hepatic abscesses.[34] In the modern era, the most common route for pyogenic liver infection is through the biliary tract, ie, ascending cholangitis. Histologically, a liver abscess is composed of a liquefied cavity filled with debris, lined by chronic inflammatory infiltrate consisting of macrophages, lymphocytes, eosinophils, and neutrophils.[33,35] Therefore, any abscess in the liver, whether pyogenic, fungal, or parasitic, may be associated with increased 18F-FDG uptake (Fig. 7A).

Echinococcus of the liver is a parasitic infection, endemic in the Mediterranean basin and other sheep-raising countries. Humans become infected by ingestion of eggs of the tapeworm *Echinococcus granulosus*, either by eating contaminated food or through contact with dogs. A hydatid cyst of echinococcal infection is composed of 3 layers. The 2 inner layers consist of the endocyst, an inner germinal layer, and the ectocyst, a translucent thin interleaved membrane. The outer pericyst consists of host inflammatory reaction producing a zone of fibroblasts, giant cells, mononuclear cells, and eosinophilic cells.[36] This inflammatory infiltrate may explain the increased uptake of 18F-FDG, which may be found in the periphery of these cysts on PET (Fig. 7B). It is yet to be determined whether uptake of 18F-FDG corresponds to disease activity in echinococcal liver infection.

The most common etiology for acute cholecystitis and ascending cholangitis is cholelithiasis. Ascending cholangitis results from bacterial infection secondary to bile stasis, usually as the result of obstruction. With the appropriate clinical setting, PET/CT images often can make the correct diagnosis of biliary inflammation rather than tumor, especially if a stone is seen on CT (Fig. 8A). Although acute pancreatitis may have multiple etiologies, the most common are cholelithiasis and alcohol abuse. After a triggering event, pancreatic inflammation occurs at the cellular level and is based on premature activation of pancreatic enzymes leading to autodigestion of the pancreatic parenchyma and peripancreatic
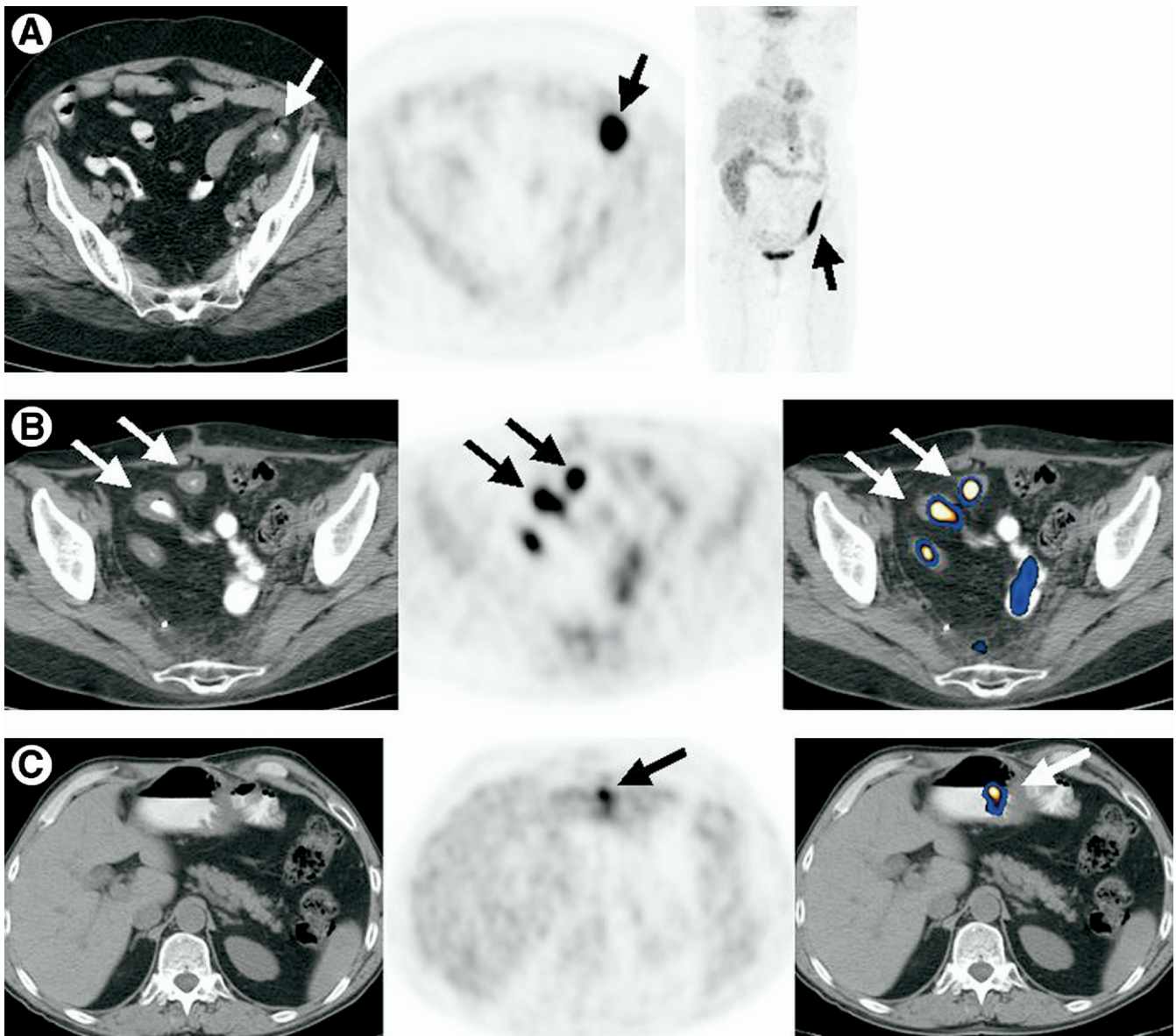
Figure 5 Inflammation along gastrointestinal tract. (A) Acute diverticulitis. Segmental, increased uptake of FDG along left colon (arrow on MIP, right image). On CT (left image) this corresponds to a thickened segment of colon, with multiple diverticula and stranding of pericolic fat (arrow), consistent with diverticulitis. (B) Crohn's disease. Abnormal uptake of FDG is seen along long segments of small bowel (arrows on middle image). On CT, these loops of small bowel appear concentrically thickened, with mild peri-enteric fat stranding and fibrofatty proliferation, consistent with Crohn's disease (confirmed on endoscopy). (C) Gastritis with gastric ulcer. On PET (middle image), marked focal uptake of FDG in antrum of stomach (arrow). On fused PET/CT (right image), this corresponds to focal thickening of stomach wall (arrow). Endoscopy showed gastritis with benign ulcer in antrum.

tissues. Perilobular or panlobular necrosis affects the acinar cells, islet cells, pancreatic ducts, and interstitial fat. Moreover, extravasation of pancreatic lipase results in the development of peripancreatic fat necrosis.[37] CT findings in pancreatitis may show diffuse or segmental enlargement of the pancreas, with obliteration of peripancreatic fat, necrosis, or pseudocyst formation. On PET/CT, these CT findings are associated with increased ^{18}F-FDG uptake (Fig. 8B).

Similar to the involvement of the liver, abscess and active granulomatous disease involving the spleen exhibit increased

uptake of ^{18}F-FDG. Granulomatous disease involving the spleen may be infectious, such as by tuberculosis or brucellosis, or inflammatory, such as by sarcoidosis. Occasionally, granulomatous disease may be suggested prospectively on whole-body imaging as the result of multisite involvement and typical imaging patterns.[38]

Inflammatory lesions involving the peritoneum and its folds harbor many pitfalls on PET/CT. When PET is performed in the immediate postoperative period, inflammatory postoperative changes may show increased uptake of
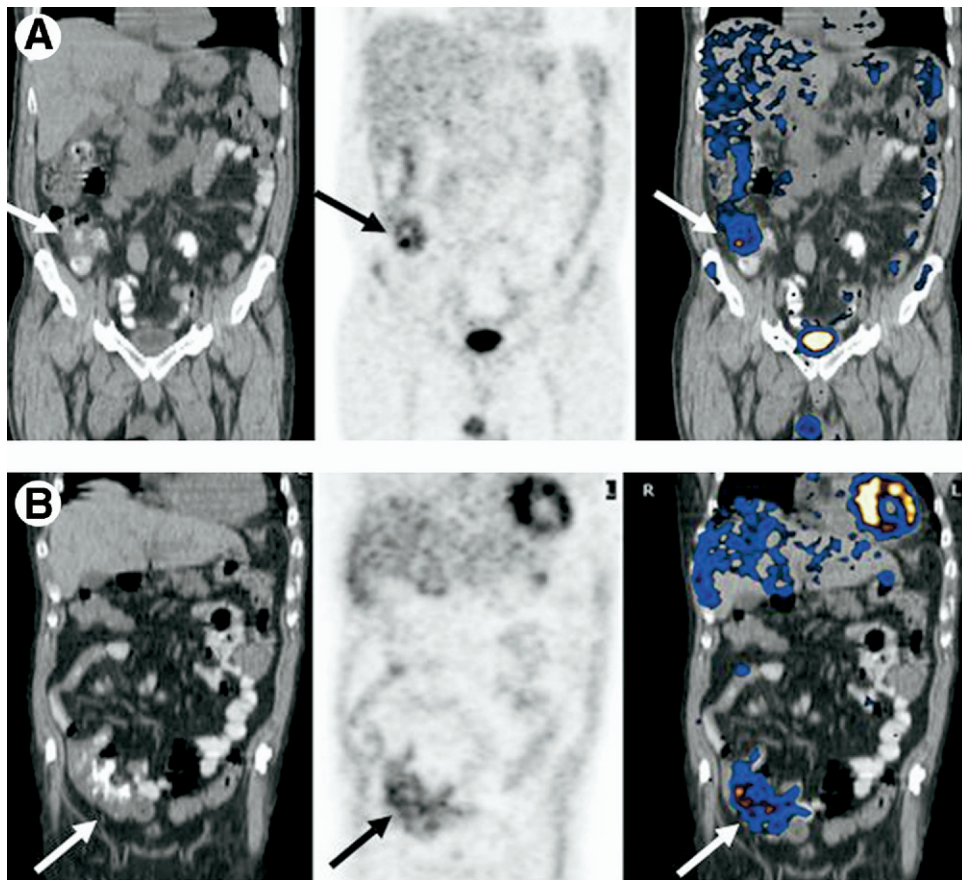
Figure 6 Bowel wall inflammation in the immuno-compromised patient. (A) Typhlitis. Mild-to-moderate uptake of FDG is seen in right colon in neutropenic patient with lymphoma after bone marrow transplantation. Colonoscopy findings were consistent with typhlitis. (B) Chronic graft-versus-host disease. Mild uptake of FDG is seen in thickened loops of small bowel. Although infectious enteritis is in the differential diagnosis, histology was consistent with chronic GVHD.

¹⁸F-FDG, indistinguishable from uptake in peritoneal malignancy (Fig. 9). This can be avoided if PET is performed at least 4 to 6 weeks after surgery. Another potential pitfall on PET is primary epiploic appendagitis (PEA). PEA results from torsion or thrombosis of one of the fatty epiploic appendages projecting from the colonic serosa, which under normal circumstances are indistinguishable from adjacent intra-abdominal fat on CT. However, after infarction, thickening of the visceral peritoneum and hazy infiltration of the fat within the appendage occur, making it visible on CT. The CT findings of PEA are sufficient for a specific diagnosis.[39] PEA may be associated with increased ¹⁸F-FDG uptake and on PET, mimicking malignancy (Fig. 10A).

Inflammation may involve the mesentery as well. Sclerosing mesenteritis is a benign process of unknown etiology affecting the small bowel mesentery. Most commonly, it is incidentally found on CT, presenting as increased attenuation mesenteric fat containing enlarged mesenteric lymph nodes. Coexisting sclerosing mesenteritis and various neoplastic diseases, most notably lymphoma, gastrointestinal tumors, and urogenital tumors, has been reported. On CT, sclerosing mesenteritis with and without tumoral involvement may appear similar.[40] Although the negative predictive

value of ¹⁸F-FDG-PET appears high, false-positive ¹⁸F-FDG-PET with moderate or marked ¹⁸F-FDG uptake may be encountered.[41]

The predominant histological changes in PEA and sclerosing mesenteritis are fat necrosis and acute inflammation. Histologically, fat necrosis is characterized by presence of foamy

Table 4 Inflammatory Lesions Showing Increased Uptake of ¹⁸F-FDG in the Liver, Gallbladder, Biliary Tree, Pancreas, Spleen, and Peritoneum

| Location	Lesion Type
Liver, gallbladder, and biliary tree	Bacterial, fungal, amebic, echinococcal abscess
	Acute cholangitis
	Acute cholecystitis
Pancreas	Acute pancreatitis
Spleen	Granulomatous infection (tuberculosis, Brucella melitensis) sarcoidosis
Peritoneum and mesentery	Peritonitis, abscess, fistula, sclerosing mesenteritis, primary epiploic appendagitis
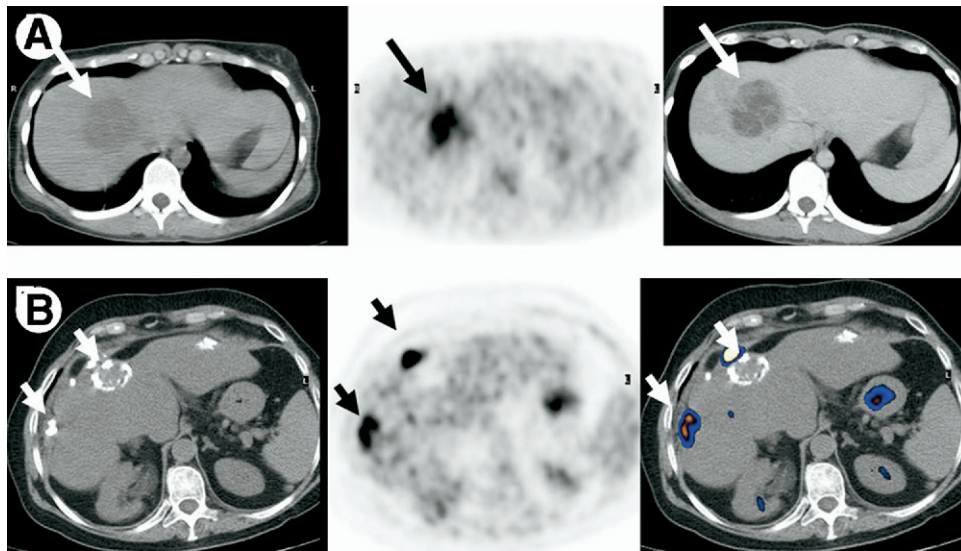
Figure 7 Liver infection. (A) Amebic abscess. Marked uptake of FDG is seen in hypoattenuating mass in anterior segment of the liver (long arrows). Contrast-enhanced CT (right image, top row) shows multiloculated fluid collection, which on aspiration was consistent with an amebic abscess. (B) Echinococcal liver cyst. Marked uptake of FDG is noted surrounding calcified masses in the periphery of the liver (short arrows on CT, left image; PET, middle image; and fused PET/CT, left image), consistent with patient's known echinococcal liver cysts.

macrophages with a surrounding inflammatory reaction. Monocytes, in general, and macrophages, in particular, are the principal ^{18}F-FDG-accumulating cells within the inflammation,[42] possibly explaining the significant accumulation of ^{18}F-FDG in processes resulting in fat necrosis. Other causes for fat necrosis may be due to release of pancreatic enzymes (secondary to pancreatitis or pancreatic surgery), or trauma,

including iatrogenic trauma. CT correlation can be used to distinguish fat necrosis from a peritoneal tumor deposit (Fig. 10B).

Radiation therapy is included in the therapeutic regimen of several abdominal and pelvic malignancies. Radiation induces inflammatory changes and increases glucose metabolism; therefore, PET generally is not performed until 2 to 3
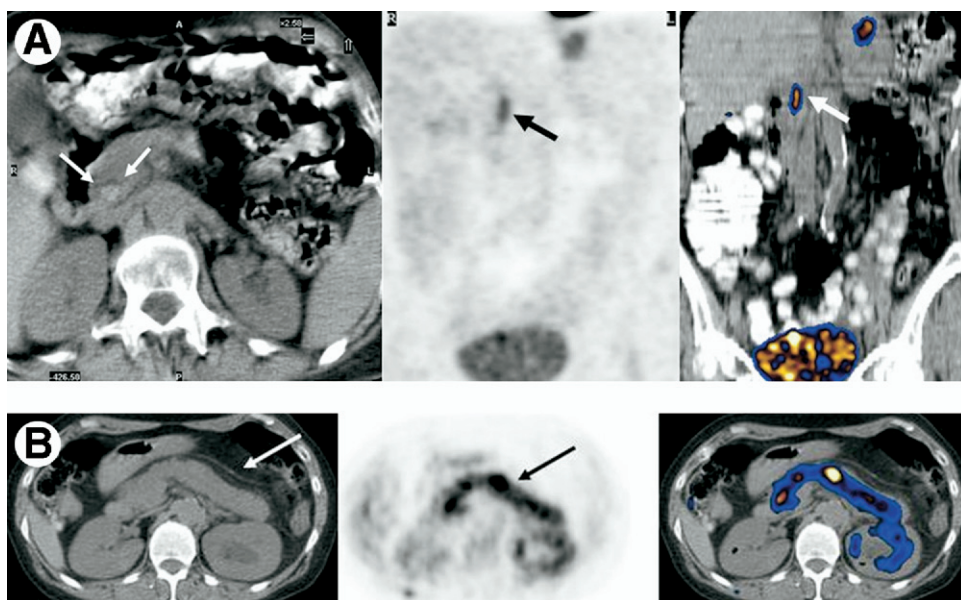

Figure 8 Acute inflammation involving biliary tract and pancreas. (A) Ascending cholangitis (top images). Axial CT image (left image) shows calculus in distal common bile duct (arrows). Coronal PET and fused images (on right) show moderate uptake of FDG is seen along common bile duct (arrow), consistent with cholangitis. (B) Acute pancreatitis. Marked uptake of FDG is observed along the pancreas on PET (arrow on middle image). On CT, the pancreas appears diffusely swollen with stranding of peripancreatic fat (arrow on left image). Increased serum amylase levels confirmed the presence of acute pancreatitis.
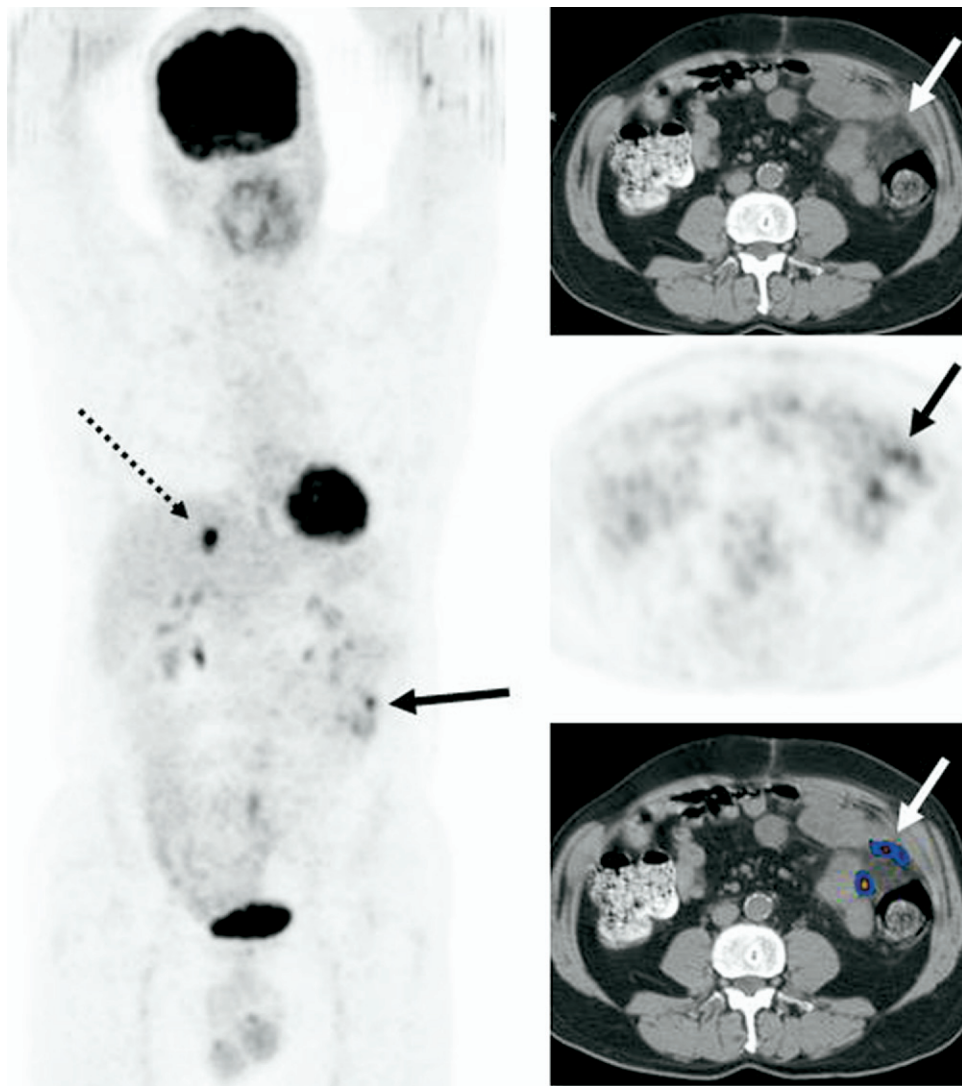
Figure 9 Postoperative omentum. PET/CT scan performed 2 weeks after resection of colon cancer. MIP image (left) shows single liver metastasis (dashed arrow), as well as moderate focal uptake in left abdomen. PET/CT images (right column: CT on top, PET in middle, fused PET/CT on bottom) show moderate focal uptake of FDG in stranding of omental fat, suggestive of postoperative change. Findings resolved on subsequent imaging.

months after radiation or chemoradiation. Nonetheless, when performed within a few weeks from completion of radiation therapy, it is often possible to differentiate between radiation-induced inflammation and residual tumor tissue.[43] In our experience, when PET is performed 6 weeks after successful radiation therapy for cervical cancer, only mild uptake of 18F-FDG is seen, likely indicating resolving radiation-induced inflammatory changes.

Genitourinary Tract (Table 5)
Although the kidneys excrete 18F-FDG, PET may detect focal cortical renal lesions with increased 18F-FDG uptake. Approximately 60% of renal cell cancers may be 18F-FDG avid[44]; however, case reports have shown that focal pyelonephritis and xanthogranulomatous pyelonephritis also may be associated with increased 18F-FDG uptake.[44,45] The pathophysiologic basis for imaging findings in acute pyelonephritis is likely multifactorial and has been previously described for

CT and magnetic resonance imaging (MRI). Histologically, focal decreased perfusion as the result of edema causes vascular compression and intravascular granulocyte aggregation. In addition, tubular obstruction caused by edema and accumulation of granulocytes result in focal decreased glomerular filtration.[46] These infiltrates of white blood cells may explain the increased 18F-FDG uptake. As the result of physiological excretion of 18F-FDG from the kidneys, these focal inflammatory renal masses may be easily overlooked on PET and easier to identify at inspection of maximum intensity projection (MIP) images, as well as fused PET/CT images (Fig. 11).

Xanthogranulomatous pyelonephritis is an uncommon chronic inflammatory process of the kidney and surrounding tissues, resulting in replacement of renal parenchyma by lipid-laden macrophages. This process is usually diffuse but rarely may be focal. Several predisposing factors have been
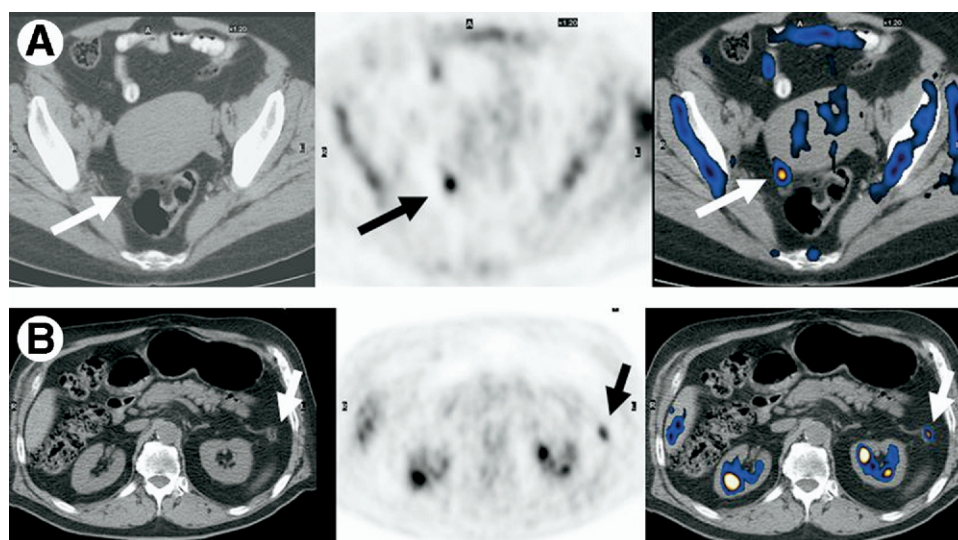
Figure 10 Inflammatory lesions in peritoneum. (A) Primary epiploic appendagitis (top images). Increased uptake of FDG is noted in a thick-walled lobule of fat as seen on CT adjacent to sigmoid colon (arrows), consistent with a torsed epiploic appendage. (B) Fat necrosis (bottom images). Increased uptake of FDG is noted in a soft-tissue nodule in left mid-abdomen, with a fat-attenuating center (arrows), suggestive of fat necrosis (biopsy proven).

described, including chronic urinary obstruction and infection and diabetes mellitus. Typical findings on CT include a diffusely enlarged kidney with multiple hypodense masses representing dilated calyces and/or cavities due to parenchymal destruction, with a contracted renal pelvis. Often, an obstructing lesion such as a staghorn calculus may also be identified. CT is particularly useful in determining the extent of the inflammatory process in perirenal tissues including the iliopsoas muscle, abdominal wall, diaphragm, skin, and bowel.[47]

An additional potential pitfall with PET imaging may be encountered in adenocarcinomas involving the lower segment of the uterine cavity, or tumors of the cervix. These tumors, when bulky, may result in endocervical stenosis and secondary fluid collections (blood or pus) in the uterine cavity.[48] This may result in increased uptake of ^{18}F-FDG along the endometrium and should not be confused with tumor extension into the uterus.

Musculoskeletal System

^{18}F-FDG-PET has been used to localize infectious processes involving the musculoskeletal system (Table 6), including chronic infections, which may be clinically challenging to diagnose.[49,50] It is especially valuable in the evaluation of the axial skeleton, where white blood-cell scans are less useful.[49] In one study of multiple myeloma patients, the use of ^{18}F-FDG-PET identified infections not detectable by other imaging modalities, even in immunosuppressed patients, accurately determined extent of infection and, on occasion, led to modification of further diagnostic workup and therapy.[50]

MRI is considered the modality of choice for early diagnosis of osteomyelitis and for the identification of associated soft-tissue abnormalities such as cellulitis, phlegmon, abscess, sinus tracts, and ulcers. However, MRI findings of acute osteomyelitis may overlap with those of neuropathic osteoarthropathy, biomechanical stress changes related to altered weight bearing, and bone marrow signal changes after orthopedic surgery or trauma.[51] Recently, ^{18}F-FDG-PET/CT has shown potential as a "single-step" imaging modality for identifying osteomyelitis of the foot in diabetic patients and in differentiating soft-tissue infection from bone involvement. Accurate registration of PET and CT data, as well as evidence of bone destruction or soft-tissue abnormality on CT, was shown to be helpful in making a confident diagnosis in this group of patients.[52]

Infection of a joint prosthesis is a serious complication, which may be difficult to differentiate from aseptic loosening. Nonetheless, this distinction is clinically relevant, as patient management of infection requires antimicrobial therapy and likely multiple surgical revisions.[53] Although it has been suggested that ^{18}F-FDG-PET is less sensitive than conventional radiography for detecting infection and performs similarly to 3-phase bone scintigraphy,[54] it appears that the negative predictive value of PET is high. Therefore, a negative PET result may eliminate the need for revision surgery.[55]

Osteoradionecrosis is potentially a significant pitfall in interpretation of ^{18}F-FDG-PET in oncology patients. The presumed mechanism for ^{18}F-FDG uptake in osteoradionecrosis

Table 5 Inflammatory Lesions Involving the Genitourinary Tract

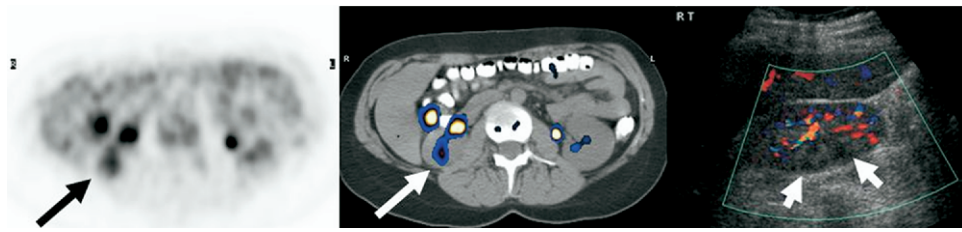| Location	Lesion Type
Kidney	Acute pyelonephritis
	Xanthogranulomatous pyelonephritis
Female genital tract	Hydrometros due to cervical stenosis
	Infected Gardner's duct cyst
Male genital tract	Epididymoorchitis prostatitis, prostatic abscess

Figure 11 Focal pyelonephritis. Moderate, focal increased uptake of FDG is noted along posterolateral aspect of right kidney (arrows on PET and fused images) in patient with fever, right flank pain, and leukocyturia. Ultrasound correlation shows area of heterogeneous echogenicity and decreased flow on Doppler, consistent with focal pyelonephritis.

is radiation-induced ischemic necrosis along with secondary inflammatory changes. The appearance of radiation necrosis on both PET and conventional imaging often may mimic a metastatic deposit and at times may show very high-level uptake of 18F-FDG.[56] Correlation with the boundaries of the radiation field and a high index of suspicion are necessary to include osteoradionecrosis in the differential diagnosis in such a clinical scenario. This diagnosis may be particularly relevant when there are no other potential sites of distant metastases and patient management may be dependent on the distinction between tumor and osteoradionecrosis.

Arthritis, whether seronegative or seropositive, can be identified on 18F-FDG-PET.[57-60] Diffuse uptake of 18F-FDG in the shoulder girdle is common, with osteoarthritis being the most common etiology. A recent study has shown that 3 PET uptake patterns may apply to 3 different entities: diffuse uptake correlates with osteoarthritis or bursitis; focal uptake at the greater tuberosity correlates with rotator cuff injury; and focal glenoid uptake correlates with frozen shoulder.[57]

In rheumatoid arthritis, 18F-FDG-PET can assess the metabolic activity of synovitis and measure disease activity. Recently, PET findings have been shown to correlate well with MRI and ultrasound assessments of the pannus in rheumatoid arthritis, as well as with serum markers of inflammation, namely, C-reactive protein, and the synovium-derived marker matrix metalloproteinase-3. The pannus is directly responsible for cartilage destruction and bone degradation, and therefore, development of bone erosions and subsequent joint narrowing (Fig. 12). Uptake of 18F-FDG is strongly correlated with clinical and laboratory parameters used for assessment of disease activity.[60] Identification of active synovitis in patients with rheumatoid arthritis is thus of utmost importance in determining treatment strategies and assessing response to therapy. In the aforementioned study, changes in SUV after 4 weeks of therapy correlated well with changes in MRI parameters and changes in serum C-reactive protein and matrix metalloproteinase-3 but not with changes in synovial thickness.[59] Although the precise mechanism for 18F-FDG uptake in rheumatoid arthritis is not completely understood, it is likely related to the presence of activated leukocytes. In addition, tumor necrosis factor-α, which bears a major role in chronic synovial inflammation, has been shown to enhance glucose entry in macrophages in experimental models of inflammation and regulates glucose transport and metabolism in fibroblasts.[10-12]

Inflammation of supporting structures, such as tendonitis or bursitis, is also commonly identified on routine whole-body 18F-FDG-PET imaging. Although not always paraneoplastic, dermatomyositis–polymyositis may indicate an increased cancer risk, especially in male patients older than 50 years of age.[61] At times, uptake of 18F-FDG may be difficult to differentiate from physiological uptake of 18F-FDG in muscles.[62] Nonetheless, dermatomyositis may show increased uptake of 18F-FDG in involved muscles.

Skin, Lymph Nodes, and Blood Vessels

There are a multitude of iatrogenic etiologies for increased uptake of 18F-FDG in the skin or subcutaneous tissue, including postoperative scar or fluid collections, or postradiation dermatitis (Table 7). Although subcutaneous injections to the abdominal wall, buttocks or thighs may usually show low-level uptake of 18F-FDG, intradermal injections of bacillus Calmette-Guérin (BCG) may show marked uptake of 18F-FDG (Fig. 13). BCG may be used as adjuvant immunotherapy in patients with melanoma and may imitate subcutaneous foci of tumor on both PET and CT. Apart from clinical

Table 6 Inflammatory Lesions Involving the Musculoskeletal System

Location	Lesion Type	
Bones and joints	Infectious	Osteomyelitis, including discitis; SAPHO syndrome
		Metallic implants (loosening, infection)
	Inflammatory	Radiation necrosis
		Osteoarthritis
		Rheumatoid arthritis
		Seronegative arthritis
Muscles and supporting structures		Bursitis
		Tendintis
		Synovitis Rotator cuff tear
		Polymyalgia rheumatica
		Myositis (infectious, paraneoplastic dermatomyositis)

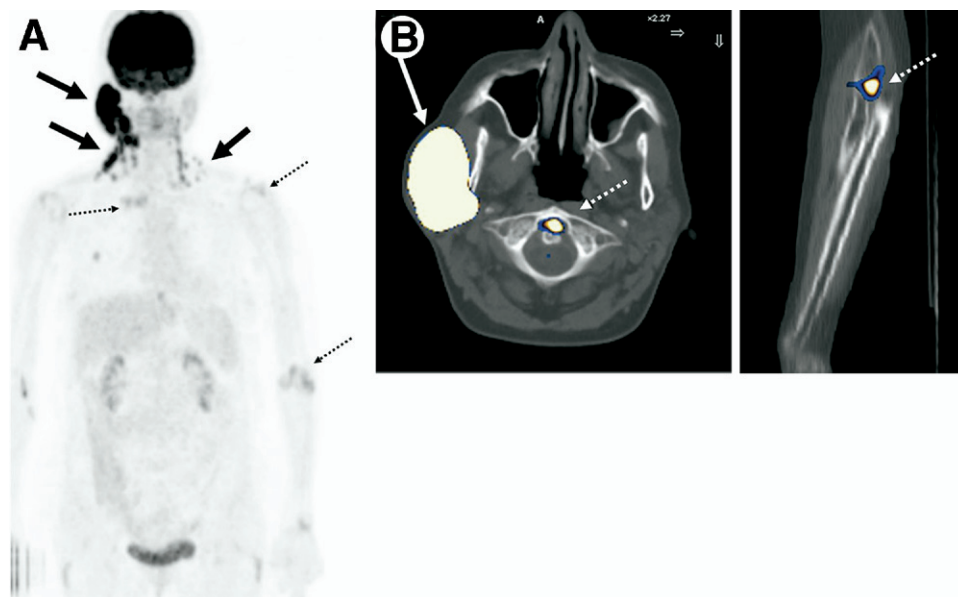SAPHO, synovitis, acne, pustulosis, hyperostosis, and osteitis.

Figure 12 Rheumatoid arthritis. (A) MIP Image. Patient with nodal lymphoma of the neck (arrows), and moderate, uptake of FDG in multiple joints (dotted arrows). (B) Fused PET/CT images show uptake in C1-C2 joint space (dotted arrow left image) and uptake in narrowed elbow joint (dotted arrow right image). On CT, joint erosions were noted. Imaging and laboratory findings were consistent with rheumatoid arthritis.

suspicion and an appropriate history, a clue to the correct diagnosis may be a symmetrical pattern of uptake, which would be unusual for tumor.

Increased ^{18}F-FDG uptake can be observed in the walls of blood vessels involved by large-vessel vasculitis, such as giant cell arteritis and Takayasu's arteritis.[63] PET can aid in accurate localization of involved sites of disease, in selecting a site for biopsy, and in follow-up after therapy.[64] Further work is needed to determine the role of PET in other vasculitides.

Reactive lymph nodes often may be encountered, secondary to localized or generalized inflammatory processes. These

nodes are responsible for decreased specificity of ^{18}F-FDG-PET nodal staging of many malignancies. In our experience, ^{18}F-FDG may show benign symmetrical perihilar uptake much like that seen on gallium-67 scintigraphy. A recent prospective study on the performance of PET/CT in staging lung cancer has shown that increased uptake of ^{18}F-FDG may be seen in nodes with calcifications (which have associated higher CT attenuation values than in the surrounding great vessels). On pathology, these nodes contained areas of mild follicular hyperplasia in the cortex and anthracotic change with pigmented macrophages and microscopic fibrotic nod-

Table 7 Inflammation Involving Skin, Lymph Nodes, and Blood Vessels

|		
Skin/subcutaneous	Post-therapy	Postoperative scar
		Postradiation
		BCG or interferon injection
	Infectious	Cellulitis, furuncle, pressure ulcer
		Herpes zoster
	Inflammatory	Granulomatous changes around surgical clips
		Eosinophilic fasciitis
		Fat necrosis
		Sarcoidosis in surgical scar
		Skin vasculitis
		Lymphedema
Lymph node		Reactive (cat scratch disease, noncaseating granuloma)
		Rosai-Dorfman disease
Blood vessels	Veins	Deep or superficial vein thrombosis
		Varicose veins
	Arteries	Atheromatous plaque
		Chronic aortic dissection
		Vasculitis
		Vascular graft (including infection)

BCG, bacillus Calmette-Guérin.
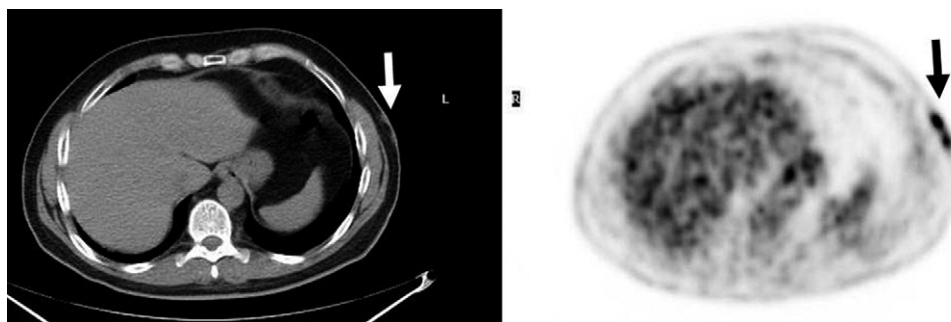
Figure 13 BCG injections. In a patient with metastatic melanoma, axial PET and CT images show marked uptake of FDG in soft-tissue attenuating nodules in the left subcutaneous fat of abdomen (arrows) caused by BCG injections.

ule formation in the medulla, consistent with reactive nodes. None of these nodes contained malignant cells.[65]

There are systemic lymph node disorders that have been shown to be 18F-FDG avid. These include Castleman's disease,[66] also known as angiofollicular or giant lymph node hyperplasia, or Rosai-Dorfman disease, a rare condition of unknown etiology. Rosai-Dorfman disease is characterized by massive, painless, lymphadenopathy with or without a low-grade fever. Extranodal involvement is possible. Usually, an indolent chronic clinical course occurs, with occasional exacerbations; however, at times a more aggressive, potentially fatal form is encountered, with destruction of osseous and soft-tissue structures. This too has been shown to be

18F-FDG avid,[67] as the result of diffuse proliferation of large histiocytic cells.

Benign Tumors and Tumor-Like Conditions

Many benign neoplasms have been shown to be 18F-FDG avid. These include pituitary adenomas, benign salivary gland tumors, thyroid adenomas, adrenal adenomas and benign pheochromocytomas, and gastrointestinal tract adenomas, among others (Table 8).[68-70] There are several benign bone lesions that show significant uptake of 18F-FDG, most notably fibrous dysplasia, enchondroma, eosinophilic granuloma (Table 9).[71] Other bone lesions, such as spurs, Schmorl's nodes, bone bridges, and exostoses may show variable uptake of 18F-FDG. Low-grade uptake of 18F-FDG may be seen in Paget's disease of the bone and should be included in the differential diagnosis for metastatic disease,[72] especially when the typical CT findings of cortical thickening, trabecular thickening, and bone enlargement are present.

Several benign, tumor-like conditions involving soft tissues may be difficult to differentiate from malignancy on PET

Table 8 Benign Tumors and Tumor-Like Conditions Showing Increased Uptake of 18F-FDG in the Head and Neck, Chest, and Abdomen

Head and neck	Pituitary	Adenoma
	Nose & nasal sinus	Inverted papilloma (nasal)
	Parapharyngeal space	Benign hemangiopericytoma
	Thyroid	Adenoma
		Multinodular goiter
Chest	Lung	Amyloidosis
	Breast	Papilloma
		Fibroadenoma
		Diabetic mastopathy
Abdomen	Liver and biliary tract	Hepatic adenoma
		Benign neuroendocrine tumor
	Gastrointestinal tract	Hyperplastic polyp, adenoma
	Spleen	Gaucher's disease
	Adrenal	Adenoma
		Benign Pheochromocytoma
	Genitourinary: female	Hemorrhagic ovarian cyst, endometrioma
		Ovarian cystadenoma
		Uterine leiomyoma
	Genitourinary: male	Prostatic adenoma

Table 9 Benign Tumors and Tumor-Like Conditions Showing Increased Uptake of 18F-FDG in the Skin and Musculoskeletal, Cardiovascular, and Nervous Systems

Skin/subcutaneous	Hibernoma
	Eosinophilic fasciitis
Musculoskeletal	Spur
	Exostosis
	Schmorl's node
	Nonossifying fibroma
	Enchondroma
	Eosinophilic granuloma
	Fibrous dysplasia
	Paget's disease
	Avascular necrosis
	Gaucher's disease
	Erdheim-Chester disease
Cardiovascular	LHIS
Nervous system	Neurofibroma
	Schwannoma

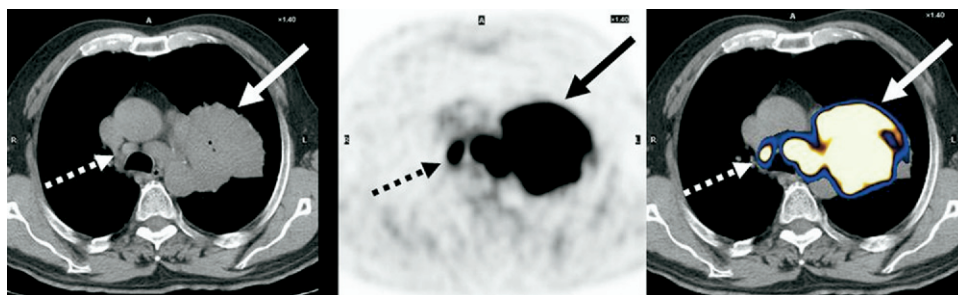LHIS, lipomatous hypertrophy of the inter-atrial septum.

Figure 14 Tumor-like conditions: pulmonary amyloidosis. Marked FDG uptake is noted in a large left upper lobe mass (arrow) and mediastinal lymph nodes (dashed arrow). Surgical pathology revealed pulmonary amyloidosis.

(Tables 8 and 9). One such entity is pulmonary amyloidosis. Amyloidosis is a disease caused by extracellular deposition of insoluble proteins. It is usually a systemic disorder and, as such, may affect the lungs in as many as half of cases. Localized forms of pulmonary amyloidosis also have been described. Chest involvement may be tracheobronchial (the most common form), with amyloidomas in the trachea or bronchi, or pulmonary, consisting of multiple or, much less commonly, solitary nodules.[73] Amyloidosis also has been shown to be ^{18}F-FDG avid and, in our experience, cannot be reliably differentiated from malignancy on PET/CT (Fig. 14).

Lipomatous hypertrophy of the interatrial septum (LHIS) of the heart is a histologically benign process in which increased adipose tissue infiltrates the interatrial septum. Most cases of LHIS have been shown to be ^{18}F-FDG avid. It has been postulated that variable presence of brown fat in LHIS may be responsible for this uptake.[74] This is also the explanation for marked uptake of ^{18}F-FDG in hibernomas, which cannot be differentiated from liposarcomas on PET/CT.[75]

Diabetic mastopathy of the breast is an uncommon tumor-like fibrous proliferation of the breast. Histologically, it consists of lymphocytic mastitis and stromal fibrosis, mostly in premenopausal women with long-standing type I diabetes mellitus. It is difficult to differentiate on imaging from malignancy. We have encountered one case of diabetic mastopathy that was ^{18}F-FDG avid. A more comprehensive analysis of this entity is needed to determine the actual avidity of this condition to ^{18}F-FDG.

Conclusion

In summary, ^{18}F-FDG is not a tumor specific agent. As such, there are many pitfalls in the reporting of oncology ^{18}F-FDG-PET studies. Although the majority of these lesions are inflammatory, some are due to benign tumors and tumor-like conditions. A thorough knowledge of these potential pitfalls is necessary to minimize false-positive ^{18}F-FDG-PET results.

References

1. Engel H, Steinert H, Buck A, et al: Whole-body PET: Physiological and artifactual fluorodeoxyglucose accumulations. J Nucl Med 37:441-446, 1996
2. Hany TF, Gharehpapagh E, Kamel EM, et al: Brown adipose tissue: A factor to consider in symmetrical tracer uptake in the neck and upper chest region. Eur J Nucl Med Mol Imaging 29:1393-1398, 2002
3. Metser U, Miller E, Lerman H, et al: Benign, non-physiologic lesions with increased ^{18}F-FDG uptake on PET/CT: Characterization and incidence. Presented at 2006 SNM Meeting, San Diego, 2006
4. Metser U, Golan O, Levine CD, et al: Tumor lesion detection: When is integrated positron emission tomography/computed tomography more accurate than side-by-side interpretation of positron emission tomography and computed tomography? J Comput Assist Tomogr 29:554-559, 2005
5. G. Antoch G, Saoudi N, Kuehl H, et al: Accuracy of whole-body dual-modality fluorine-18-2-fluoro-2-deoxy-D-glucose positron emission tomography and computed tomography (FDG-PET/CT) for tumor staging in solid tumors: Comparison with CT and PET. J Clin Oncol 22:4357-4368, 2004
6. Pelosi E, Messa C, Sironi S, et al: Value of integrated PET/CT for lesion localisation in cancer patients: A comparative study. Eur J Nucl Med Mol Imaging 31:932-939, 2004
7. Reinartz P, Wieres FJ, Schneider W, et al: Side-by-side reading of PET and CT scans in oncology: Which patients might profit from integrated PET/CT? Eur J Nucl Med Mol Imaging 31:1456-1461, 2004
8. Roitt IM, Delves PJ: Lymphocyte activation, in Roitt IM (ed): Essential Immunology (ed 10). Blackwell Scientific, Oxford, UK, 2001, pp 164–176
9. Kubota R, Yamada S, Kubota K, et al: Intratumoral distribution of fluorine-18-fluorodeoxyglucose in vivo: High accumulation in macrophages and granulation tissues studied by microautoradiography. J Nucl Med 33:1972-1980, 1992
10. Gamelli RL, Liu H, He LK, et al: Augmentations of glucose uptake and glucose transporter-1 in macrophages following thermal injury and sepsis in mice. J Leukoc Biol 59:639-647, 1996
11. Fukuzumi M, Shinomya H, Shimizu Y, et al: Endotoxin-induced enhancement of glucose influx into murine peritoneal macrophages via Glut1. Infect Immun 64:108-112, 1996
12. Paik JY, Lee KH, Choe YS, et al: Augmented 18F-FDG uptake in activated monocytes occurs during the priming process and involves tyrosine kinases and protein kinase C. J Nucl Med 45:124-128, 2004
13. Babior BM: The respiratory burst of phagocytes. J Clin Invest 73:599-601, 1984
14. Yamada Y, Uchida Y, Tatsumi K, et al: Fluorine-18-fluorodeoxyglucose and carbon-11-methionine evaluation of lymphadenopathy in sarcoidosis. J Nucl Med 39:1160-1166, 1998
15. Walter MA, Melzer RA, Schindler C, et al: The value of [18F]FDG-PET in the diagnosis of large-vessel vasculitis and the assessment of activity and extent of disease. Eur J Nucl Med Mol Imaging 32:674-681, 2005
16. Mahfouz T, Miceli MH, Saghafifar F, et al: ^{18}F-fluorodeoxyglucose positron emission tomography contributes to the diagnosis and management of infections in patients with multiple myeloma: A study of 165 infectious episodes. J Clin Oncol 23:7857-7863, 2005
17. Rice DH: Diseases of the salivary glands-non-neoplastic, in Bailey BJ et al (eds), Head and Neck Surgery-Otolaryngology (ed 2). JB Lippincott, Philadelphia, PA, 1933, pp 19-37
18. Andrade RS, Heron DE, Degirmenci B, et al: Posttreatment assessment of response using FDG-PET/CT for patients treated with definitive ra-

diation therapy for head and neck cancers. Int J Radiat Oncol Biol Phys 65:1315-1322, 2006

19. Asad S, Aquino SL, Piyavisetpat N, et al: False-positive FDG positron emission tomography uptake in nonmalignant chest abnormalities. AJR Am J Roentgenol 182:983-989, 2004

20. Wheeler PS, Stitik FP, Hutchins GM, et al: Diagnosis of lipoid pneumonia by computed tomography. JAMA 245:65-66, 1981

21. Tahon F, Berthezene Y, Hominal S, et al: Exogenous lipoid pneumonia with unusual CT pattern and FDG positron emission tomography scan findings. Eur Radiol 12:S171-173, 2002

22. Brauner MW, Grenier P, Mouelhi MM, et al: Pulmonary histiocytosis X: Evaluation with high-resolution CT. Radiology 172:255-258, 1989

23. Kamel EM, McKee TA, Calcagni ML, et al: Occult lung infarction may induce false interpretation of 18F-FDG PET in primary staging of pulmonary malignancies. Eur J Nucl Med Mol Imaging 32:641-646, 2005

24. Rossi SE, Erasmus JJ, McAdams HP, et al: Pulmonary drug toxicity: radiologic and pathologic manifestations. RadioGraphics 20:245-1259, 2000

25. Shin L, Katz DS, Yung E: Hypermetabolism on F-18 FDG PET of multiple pulmonary nodules resulting from bronchiolitis obliterans organizing pneumonia. Clin Nucl Med 29:654-656, 2004

26. Lee KS, Kullnig P, Hartmanet TE, et al: Cryptogenic organizing pneumonia: CT findings in 43 patients. AJR Am J Roentgenol 162:543-554, 1994

27. Lynch DA, Travis WD, Muller NL, et al: Idiopathic interstitial pneumonias: CT features. Radiology 236:10-21, 2005

28. Messner HH, Soo Hoo GW, Khonsary SA, et al: Idiopathic pulmonary fibrosis: Evaluation with positron emission tomography. Respiration 73:197-202, 2006

29. Hassaballa HA, Cohen ES, Khan AJ, et al: Positron emission tomography demonstrates radiation-induced changes to nonirradiated lungs in lung cancer patients treated with radiation and chemotherapy. Chest 128:1448-1452, 2005

30. Tatlidil R, Jadvar H, Bading JR, et al: Incidental colonic fluorodeoxyglucose uptake: Correlation with colonoscopic and histopathologic findings. Radiology 224:783-787, 2002

31. Frick MP, Maile CW, Crass JR, et al: Computed tomography of neutropenic colitis. AJR Am J Roentgenol 143:763-765, 1984

32. Donnelly LF, Morris CL: Acute graft-versus-host disease in children: Abdominal CT findings. Radiology 199:265-268, 1996

33. Samuelson J, Von Lichtenberg F: Infectious diseases, in: Cotran RS, Kumar V, Robbins SL (eds): Pathologic basis of disease (ed 5). Philadelphia, Saunders, 1994, pp 305-377

34. Mergo PJ, Ros PR: MR imaging of inflammatory disease of the liver. Magn Reson Imaging Clin N Am 5:367-376, 1997

35. Huang CJ, Pitt HA, Lipsett PA, et al: Pyogenic hepatic abscess. Ann Surg 223:600-609, 1996

36. Von Lichtenberg F: Infectious diseases, in Cotran RS, Kumar V, Robbins SL (eds): Pathologic basis of disease (ed 3). Philadelphia, Saunders, 1984, pp 385-386

37. Balthazar EJ: Acute pancreatitis: Assessment of severity with clinical and CT evaluation. Radiology 223:603-613, 2002

38. Metser U, Miller E, Kessler A, et al: Solid splenic masses: evaluation with 18F-FDG PET/CT. J Nucl Med 46:52-59, 2005

39. Rao PM, Wittenberg J, Lawrason JN: Primary epiploic appendagitis: Evolutionary changes in CT appearance. Radiology 204:713-717, 1997

40. Horton KM, Lawler LP, Fishman EK: CT findings in sclerosing mesenteritis (panniculitis): Spectrum of disease. Radiographics 23:1561-1567, 2003

41. Zissin R, U. Metser U, Hain D, et al: Mesenteric panniculitis in oncologic patients: PET-CT findings. Br J Radiol 79:37-43, 2006

42. Deichen JT, Prante O, Gack M, et al: Uptake of [¹⁸F]fluorodeoxyglucose in human monocyte-macrophages in vitro. Eur J Nucl Med Mol Imaging 30:267-273, 2003

43. Weber WA: Use of PET for monitoring cancer therapy and for predicting outcome. J Nucl Med 46:983-995, 2005

44. Ak I, Can C: F-18 FDG PET in detecting renal cell carcinoma. Acta Radiol 46:895-899, 2005

45. Swingle CA, Baumgarten DA, Schuster DM: Xanthogranulomatous pyelonephritis characterized on PET/CT. Clin Nucl Med 30:728-729, 2005

46. Majd M, Nussbaum Blask AR, Markle BM, et al: Acute pyelonephritis: comparison of diagnosis with 99mTc-DMSA, SPECT, spiral CT, MR imaging, and power Doppler US in an experimental pig model. Radiology 218:101-108, 2001

47. Hayes WS, Hartman DS, ISesterbenn IA: From the Archives of the AFIP: Xanthogranulomatous pyelonephritis. Radiographics 11:485-498, 1991

48. Walsh JW: Computed tomography of gynecologic neoplasms. Radiol Clin North Am 30:817-818, 1992

49. de Winter F, van de Wiele C, Vogelaers D, et al: Fluorine-18 fluorodeoxyglucose-position emission tomography: a highly accurate imaging modality for the diagnosis of chronic musculoskeletal infections. J Bone Joint Surg Am 83:651-660, 2001

50. Mahfouz T, Miceli MH, Saghafifar F, et al: 18F-fluorodeoxyglucose positron emission tomography contributes to the diagnosis and management of infections in patients with multiple myeloma: A study of 165 infectious episodes. J Clin Oncol 23:7857-7863, 2005

51. Schweitzer ME, Morrison WB: MR imaging of the diabetic foot. Radiol Clin North Am 42:61-71, 2004

52. Keidar Z, Militianu D, Melamed E, et al: The diabetic foot: initial experience with 18F-FDG PET/CT. J Nucl Med 46:444-449, 2005

53. Harkess JW: Arthroplasty of hip, in Canale ST (ed): Campbell's Operative Orthopaedics (ed 9). St. Louis, Mosby, 1998, pp 296-456

54. Stumpe KD, Notzli HP, Zanetti M, et al: FDG PET for differentiation of infection and aseptic loosening in total hip replacements: comparison with conventional radiography and three-phase bone scintigraphy. Radiology 231:333-341, 2004

55. Delank KS, Schmidt M, Michael JW, et al: The implications of 18F-FDG PET for the diagnosis of endoprosthetic loosening and infection in hip and knee arthroplasty: Results from a prospective, blinded study. BMC Musculoskelet Disord 7:20, 2006

56. Liu SH, Chang, JT Ng SH, et al: False positive fluorine-18 fluorodeoxy-D-glucose positron emission tomography finding caused by osteoradionecrosis in a nasopharyngeal carcinoma patient. Br J Radiol 77:257-260, 2004

57. Wandler E, Kramer EL, Sherman O, et al: Diffuse FDG shoulder uptake on PET is associated with clinical findings of osteoarthritis. AJR Am J Roentgenol 185:797-803, 2005

58. Wendling D, Blagosklonov O, Streit G, et al: FDG-PET/CT scan of inflammatory spondylodiscitis lesions in ankylosing spondylitis, and short term evolution during anti-tumour necrosis factor treatment. Ann Rheum Dis 64:1663-1665, 2005

59. Beckers C, Jeukens X, Ribbens C, et al: (18)F-FDG PET imaging of rheumatoid knee synovitis correlates with dynamic magnetic resonance and sonographic assessments as well as with the serum level of metalloproteinase-3. Eur J Nucl Med Mol Imaging 33:275-280, 2006

60. Beckers C, Ribbens C, Andre B, et al: Assessment of disease activity in rheumatoid arthritis with (18)F-FDG PET. J Nucl Med 45:956-964, 2004

61. Campanella N, Moraca A, Pergolini M, et al: Paraneoplastic syndromes in 68 cases of resectable non-small cell lung carcinoma: Can they help in early detection? Med Oncol 16:129, 1999

62. Herder GJ, Welling A, De Winter GV, et al: Accessory findings on F-18 FDG positron emission tomography in bronchogenic carcinoma. Clin Nucl Med 28:58-59, 2003

63. Blockmans D, Stroobants S, Maes A, et al: Positron emission tomography in giant cell arteritis and polymyalgia rheumatica: Evidence for inflammation of the aortic arch. Am J Med 108:246-249, 2000

64. Kobayashi Y, Ishii K, Oda K, et al: Aortic wall inflammation due to Takayasu arteritis imaged with 18F-FDG PET coregistered with enhanced CT. J Nucl Med 46:917-922, 2005

65. Shim SS, Lee KS, Kim BT, et al: Non-small cell lung cancer: Prospective comparison of integrated FDG PET/CT and CT alone for preoperative staging. Radiology 236:1011-1019, 2005

66. Reddy MP, Graham MM: FDG positron emission tomographic imaging of thoracic Castleman's disease. Clin Nucl Med 28:325-326, 2003

67. Lim R, Wittram C, Ferry JA, et al: FDG PET of Rosai-Dorfman disease of the thymus. AJR Am J Roentgenol, 182:514, 2004

68. De Souza B, Brunetti A, Fulham MJ, et al: Pituitary microadenomas: A PET study. Radiology 177:39-44, 1990

69. Metser U, Miller E, Lerman H, et al: 18F-FDG PET/CT in the evaluation of adrenal masses. J Nucl Med 47:32-37, 2006

70. Yasuda S, Fujii H, Nakahara T, et al: 18F-FDG PET detection of colonic adenomas. J Nucl Med 42:989-992, 2001
71. Aoki J, Watanabe H, Shinozaki T, et al: FDG PET of primary benign and malignant bone tumors: standardized uptake value in 52 lesions. Radiology 219:774-777, 2001
72. Watanabe H, Shinozaki T, Yanagawa T, et al: Grading of tumors and tumorlike lesions of bone: Evaluation by FDG PET. J Nucl Med 41: 1695-1701, 2000
73. Urban BA, Fishman EK, Goldman SM, et al: CT evaluation of amyloidosis: Spectrum of disease. Radiographics 13:1295-1308, 1993
74. Fan CM, Fischman AJ, Kwek BH, et al: Lipomatous hypertrophy of the interatrial septum: increased uptake on FDG PET. AJR Am J Roentgenol 184:339-342, 2005
75. Tsuchiya T, Osanai T, Ishikawa A, et al: Hibernomas show intense accumulation of FDG positron emission tomography. J Comput Assist Tomogr 30:333-336, 2006